BUILD SIMUL (2019) 12: 723–734
https://doi.org/10.1007/s12273-019-0522-8

Particle deposition in ventilation ducts: A review

Hao Lu[1] (✉), Yuanhao Wang[2] (✉)

1. Key Laboratory of Enhanced Heat Transfer and Energy Conservation of Education Ministry, School of Chemistry and Chemical Engineering, South China University of Technology, Guangzhou 510640, China

2. Faculty of Science and Technology, Technological and Higher Education Institute of Hong Kong, New Territories, Hong Kong, China

Review Article

Abstract

This paper reviewed particle deposition behaviors and mechanisms in turbulent ventilation duct flows. The main theoretical prediction models, experimental techniques and numerical methods used to explore particle deposition were discussed and analyzed. It was observed that turbophoresis, Brownian diffusion, turbulent diffusion and gravitational settling are the main mechanisms of particle deposition in smooth duct flows. The important factors influencing particle deposition behaviors and mechanisms are duct inclination angle, thermophoresis, electrophoresis and surface ribs. Numerical simulation was shown to be the main tool used to investigate complex particle deposition in turbulent duct flows. However, it is necessary to develop accurate experimental measures of particle deposition in complex turbulent duct flows.

Keywords

particle deposition,
turbulent duct flow,
inclination angle,
thermophoresis,
electrophoresis,
surface ribs

Article History

Received: 21 October 2018
Revised: 26 January 2019
Accepted: 29 January 2019

Indoor/Outdoor Airflow and Air Quality

1 Introduction

Particulate matter (PM) in the air can be inhaled into the lungs that causes damages to human health (Zhai and Jin 2018; Wu et al. 2018; Zhao et al. 2005). In recent years, air pollution by PM has become an extremely serious problem in industrial regions such as northern China (Chen and Zhang 2005; Blocken 2018; Zhao and Zhao 2018). Therefore, particle deposition in airflows has recently begun to attract much research attention, with a large number of studies conducted on this important issue (Gao et al. 2018; Nazaroff 2008; Wang and Chen 2007; Tian et al. 2007; Zhao et al. 2008; Sun et al. 2007). Understanding particle deposition behaviors and mechanisms in turbulent duct flows is crucial to a wide range of industrial processes, such as building ventilation duct system, particle removal devices and air cleaner (Kato and Yang 2008). In built environments, particle deposition processes in ventilation duct systems are extremely important to indoor air quality. The airflow in building ventilation ducts is commonly turbulent. Particle dispersion and deposition in ventilation ducts are complicated processes influenced by a large number of factors, such as gravity settling, Brownian diffusion, turbulent flow structures and turbophoresis. Therefore, it is necessary to review the progress made by studies of particle deposition in turbulent duct flows to support future engineering applications and research.

Most of the research on this important issue has focused on particle deposition in smooth and vertical duct airflows without considering thermophoresis or electrophoresis. Figure 1 shows particle deposition velocity profiles for smooth and vertical duct airflows obtained by theoretical, experimental and numerical methods (Wood 1981; Friedlander and Johnstone 1957; Postma and Schwendiman 1960; Well and Chamberlain 1967; Liu and Agarwal 1974; El-Shobokshy 1983; Sehmel 1970; Shimada et al. 1993; Lee and Gieseke 1994; Tian and Ahmadi 2007; Zhang and Chen 2007; Lu and Lu 2015a). Dimensionless particle deposition velocity is normalized by flow frictional velocity. Wood (1981) proposed that particle deposition in vertical ducts can be divided into

E-mail: luhao@scut.edu.cn (Hao Lu); wangyuanhao@vtc.edu.hk (Yuanhao Wang)

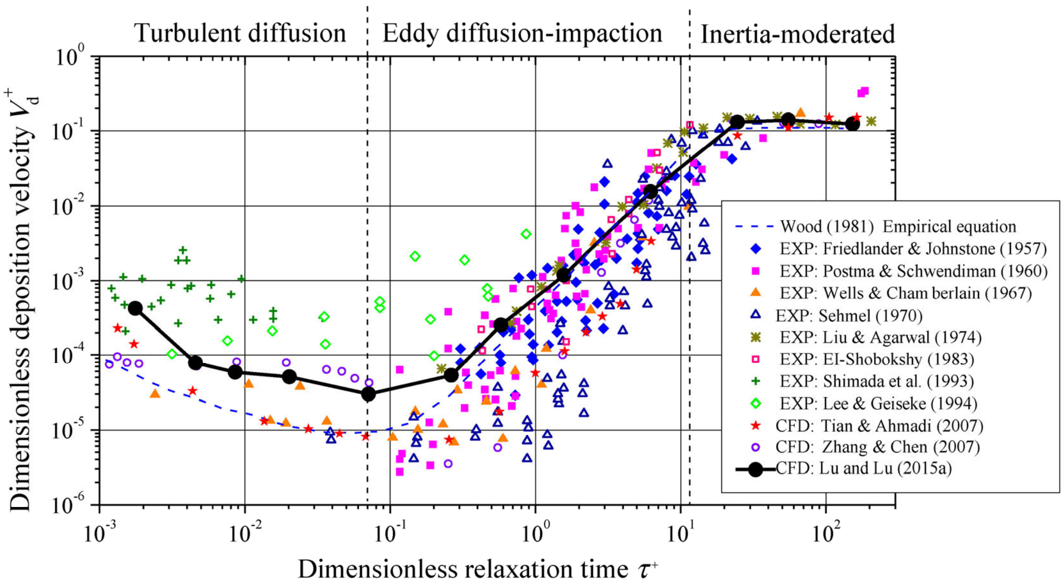

Fig. 1 Particle deposition velocity in smooth and vertical duct airflows (Lu and Lu 2015a; reproduced with permission ©Elsevier)

three regimes: a turbulent particle diffusion regime, an eddy diffusion-impaction regime and an inertia-moderated regime. In the first regime, particle deposition velocity is mainly determined by turbulent eddy diffusion and Brownian diffusion when the particle relaxation time is short. Particle deposition velocity decreases as particle relaxation time increases. In the second regime, particle deposition is controlled mainly by a combination of turbulent eddy diffusion and particle inertia. Particle deposition velocity increases greatly by three to four orders of magnitude in the eddy diffusion-impaction regime. In the last regime, particle inertia is the main mechanism of deposition at long particle relaxation times. Particle deposition velocity remains roughly constant as particle relaxation time increases.

In recent years, particle deposition in complicated duct airflows has been investigated in a number of studies based on the above basic set of particle deposition processes. Important topics such as the effects of duct inclination angle, thermophoresis, electrophoresis and surface ribs on particle deposition velocities and behaviors have been explored. Although two reviews of research on particle deposition have been conducted to date, one by Lai (2002) on indoor environments and the other by Guha (2008) on laminar and turbulent flows, no comprehensive review of particle deposition focusing on research methods and complicated turbulent duct flows has yet been carried out. Yet a large number of studies have been conducted and considerable progress has been made in the area of particle deposition in turbulent duct flows in recent years. This review presents the theoretical, experimental and numerical progress made by research on particle deposition in complicated turbulent duct flows. The limitations of previous studies and directions for future research are also discussed.

2 Research methodology

Theoretical analysis, experimental studies and numerical simulation are the three main methods used to investigate particle deposition in turbulent duct flows. In this section, each of these three methods and their key findings are described.

2.1 Theoretical analysis

The main mechanisms of particle deposition in turbulent duct flows are gravitational settling, turbophoresis, Brownian diffusion and turbulent diffusion (Lai and Nazaroff 2000). Most theoretical models of particle deposition in duct flow have been based on these mechanisms (Zhao and Wu 2006a,b; Lai 2005; Lai and Nazaroff 2005; Piskunov 2009; Nazaroff 2004). The three-layer particle deposition model proposed by Lai and Nazaroff (2000) is one of the most successful and representative theoretical prediction models. This Eulerian model is predicated on the assumption that the particle concentration layer within the turbulent boundary layer is extremely thin. The original three-layer model is based on Fick's law and considers Brownian diffusion, turbulent diffusion and gravitational settling, as shown in Eq. (1):

$$J = -\left(\varepsilon_p + D\right)\frac{\partial C}{\partial y} - iv_s C \qquad (1)$$

where J is the particle flux to the surface and D is the particle Brownian diffusivity in the boundary layer, which can be calculated as follows:

$$D = \frac{k_B T C_c}{3\pi\mu d_p} \tag{2}$$

where C is the mean concentration of the particles, y is the distance to the surface in the normal direction and v_s is the settling velocity of the particles, which is computed as follows:

$$|v_s| = C_c\left[\frac{4}{3}\cdot\frac{g\cdot d_p}{C_D}\frac{(\rho_p-\rho)}{\rho}\right]^{1/2} \tag{3}$$

where i represents the orientation of the surface. If the surface is horizontal and upward facing, $i = 1$. If the surface is horizontal and downward facing, $i = -1$. If the surface is vertical, $i = 0$. ε_p is the eddy diffusivity of particles in the boundary layer. In Lai and Nazaroff (2000)'s model, particle eddy diffusivity, ε_p, equals the turbulent viscosity of the fluids, ν_t. The turbulent viscosity of the fluids can be estimated using the direct numerical simulation (DNS) results. The fitted equation for ν_t is integrated by three y^+ intervals, as shown in Eq. (2):

$$\begin{cases} \nu_t/\nu = 7.669\times10^{-4}(y^+)^3 & 0\le y^+\le 4.3 \\ \nu_t/\nu = 1.00\times10^{-3}(y^+)^{2.8214} & 4.3\le y^+\le 12.5 \\ \nu_t/\nu = 1.07\times10^{-2}(y^+)^{1.8895} & 12.5\le y^+\le 30 \end{cases} \tag{4}$$

However, particle turbophoresis is not considered in Lai and Nazaroff (2000)'s model. Therefore, Zhao and Wu (2006a) modified the three-layer model to accommodate particle turbophoresis, as shown in Eq. (5).

$$J = -(\varepsilon_p + D)\frac{\partial C}{\partial y} - i v_s C + V_t C \tag{5}$$

The deposition velocity caused by turbophoresis can be characterized by V_t. Caporaloni et al. (1975) calculated particle turbophoretic velocity as follows:

$$V_t = -\tau_p\frac{\mathrm{d}\overline{v_{py}'^2}}{\mathrm{d}y} \tag{6}$$

In addition, Zhao and Wu (2006a) modified the eddy diffusivity of particles, ε_p, as shown in Eq. (7). The modified three-layer model for smooth duct airflow is represented in Eq. (8). More details of the development of the three-layer model can be found in the literature (Lai and Nazaroff 2000; Zhao and Wu 2006a). Generally, the modified three-layer model accurately predicts particle deposition velocity in fully developed and smooth turbulent duct flows. However, accurately modeling particle deposition velocity in complicated duct flows is quite challenging, because the eddy diffusivity of particles in complicated turbulent flows is difficult to fit.

$$\varepsilon_p = \left(1+\frac{\tau_p}{\tau_L}\right)^{-1}\nu_t \tag{7}$$

$$J_{(u^*,d_p)} = -\left(\frac{\tau_L}{\tau_p+\tau_L}\nu_t + \frac{k_B T C_c}{3\pi\mu d_p}\right)\frac{\partial C}{\partial y} - iC_c\left[\frac{4}{3}\cdot\frac{g\cdot d_p}{C_D}\frac{(\rho_p-\rho)}{\rho}\right]^{1/2} C - \tau_p\frac{\mathrm{d}\left[\frac{\tau_L}{\tau_p+\tau_L}\overline{v_y'^2}\right]}{\mathrm{d}y}C \tag{8}$$

The summary of theoretical models on predicting particle deposition in ventilation duct flow can be seen in the Table 1.

2.2 Experimental studies

Experimentally measuring particle deposition velocity in turbulent duct flows is crucial to validate the results of theoretical models and numerical simulation. However, this is extremely challenging due to the complexities of turbulent flow fields and particle motion behaviors. Generally, two main methods have been used to measure particle deposition rate in turbulent duct flows: direct measurement and indirect measurement (Roff 1994; Hahn et al. 1985; Lai et al 1999, 2000, 2001, 2002; Jiang et al. 2011; Sun et al. 2013; Sun and Lu 2013).

The fluorescence spectroscopy method (Roff 1994) and neutron activation analysis (Hahn et al. 1985) are the most common methods of directly measuring particle deposition. Lai et al. (1999) indicated that the fluorescence spectroscopy method has two major weaknesses: deposited particles can be removed from the test surface and the spatial distribution of deposited particles cannot be obtained. Neutron activation analysis is a semi-invasive particle detection technique with

Table 1 Theoretical models for particle deposition in ventilation duct flow

Theoretical model for particle deposition	The proposers	Deposition mechanisms
Diffusion model	Adolf Fick (Lai and Nazaroff 2000)	Fick diffusion
The three-layer model	Lai and Nazaroff (2000)	Brownian diffusion, turbulent diffusion and gravitational settling
The revised three-layer model	Zhao and Wu (2006a)	Brownian diffusion, turbulent diffusion, gravitational settling and turbophoresis

high sensitivity. Deposited particles need not be removed from the test surface using this method.

In terms of indirect measurement, particle deposition velocity is commonly inferred from upstream and downstream particle concentrations. Direct techniques for measuring particle deposition velocity are more reliable and sensitive than indirect measures, because small errors in particle concentration measurement may induce a large deviation in particle deposition velocity. Particle counting is the most common means of measuring airborne particle concentration (Jiang et al. 2001; Sun et al. 2013; Sun and Lu 2013). The typical test rig for measuring particle deposition in a 90° bend by Sun et al. (2013) can be seen in Fig. 2. The measuring procedures are as follows: Airflow was generated by a stable centrifugal fan. The air velocity can be adjusted by using the speed controller. A spiral-wound flexible duct was used to connect the fan and test duct to decrease the transmission vibrations. The air firstly flows through a particle filter to remove the existed dust and then passes through a grid to reduce flow turbulence. The distance between the fan and test position should be long enough to make sure the full development of turbulent airflow. Tested particles were released after the grid by the PALAS disperser (RBG1000) at a uniform feeding rate. The Arizona test particles (ISO 12103–1A2) were used to fit the real aerosol particles in Sun's experiments. The airflow velocity was measured by a TSI anemometer (Model 8386A). The particle concentrations before and after the bend can be measured by a particle counter (LASAIR II 310A). Then the particle deposition efficiency can be calculated by,

$$\eta = (1-P)\times 100\% = \frac{C_{\mathrm{i}} - C_0}{C_{\mathrm{i}}} \tag{9}$$

Stable and constant particle airflow fields must be obtained before using the particle counting technique; otherwise, the uncertainty and error associated with the particle concentration measurement will be very large. In addition to measurement techniques, airflow fields and particle samples are crucial to the accurate investigation of particle deposition rate in turbulent duct flows. Airflow fields must be highly stable and constant. In addition, particle samples should be highly monodispersed, because particle size has an important influence on aerosol deposition velocities and behaviors. Due to the challenges involved in accurately measuring particle deposition, few experimental studies of particle deposition in turbulent duct flows have been conducted to date. In recent years, studies of particle deposition in duct flows have addressed more complicated physical processes, such as thermophoresis or electrophoresis, and more complex duct geometry, such as ribbed ducts or rough ducts. However, the main investigation methods have been numerical simulation and theoretical analysis. Future researchers are urged to experimentally measure and validate particle deposition in complicated duct flows.

2.3 Numerical simulation

Numerical simulation is now the most widely used approach to investigating particle deposition in turbulent duct flows, especially in complicated cases of duct flow. Chen (2009)'s

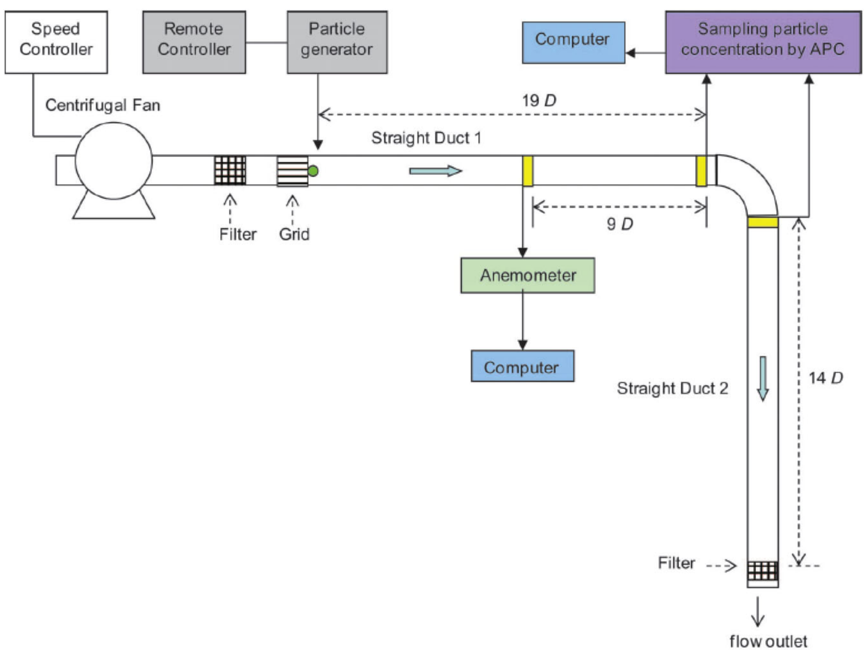

Fig. 2 Schematic diagram of the experimental measurement for particle deposition in a 90° bend (Sun et al. 2013; reproduced with permission ©Taylor & Francis)

review indicated that more than 70% of building ventilation performance studies in 2007 were based on numerical simulation, making it easy for researchers to obtain all of the relevant details of turbulent flow fields and particle deposition behaviors (Ounis et al. 1993; Zhang and Ahmadi 2000; Lai and Chen 2006; Li and Ahmadi 1992; Kallio and Reeks 1989). It would be much more challenging to obtain this information via other methods, such as experimental measurement or theoretical analysis. For example, it is quite difficult to accurately measure and analyze particle deposition and behaviors in the near-wall region through experiments.

To accurately predict particle deposition behaviors, it is crucial to establish suitable numerical models for different particulate flow conditions. Eulerian-Lagrangian frames are widely considered to offer a powerful tool for modeling particle deposition in turbulent duct flows. These frames were used to model the particle deposition process in smooth duct flows by Tian and Ahmadi (2007), Zhang and Chen (2007), Gao and Niu (2007), Gao et al. (2012), Jiang et al. (2010, 2012) Li and Ahmadi (1992, 1993, 1995) and Sun et al. (2011a,b; 2012). In a Eulerian-Lagrangian frame, airflow in a duct is considered a continuous phase, whereas aerosol particles are treated as a discrete phase. Turbulent airflow fields are resolved and obtained by computational fluid dynamics, and particle behaviors are tracked using Newton's second law equations. The accurate simulation of turbulent duct flow is crucial to the further prediction of particle deposition behaviors. DNS and large eddy simulation (LES) yield accurate turbulent flow fields and detailed turbulent structures, but incur a fairly high computational cost in engineering applications, especially when the duct flow has a high Reynolds number. Tian and Ahmadi (2007) simulated particle deposition in turbulent duct flows using different Reynolds-average Navier-Stokes (RANS) methods. The results showed that the Reynolds stress model (RSM) with correction for turbulent fluctuation more accurately predicted particle deposition behaviors and velocities than other RANS models, such as the k-ε and k-ω turbulence models. The RSM model considered turbulent anisotropy, whereas the other eddy viscosity models assumed that turbulent structures are isotropic. The mean Navier-Stokes equations for RSM model can be described by,

$$\frac{\partial \bar{u}_i}{\partial x_i} = 0 \tag{10}$$

$$\frac{\partial \bar{u}_i}{\partial t} + \bar{u}_j \frac{\partial \bar{u}_i}{\partial x_j} = -\frac{1}{\rho}\frac{\partial \bar{p}}{\partial x_i} + \frac{1}{\rho}\frac{\partial}{\partial x_j}\left(\mu \frac{\partial \bar{u}_i}{\partial x_j} - \rho \overline{u_i' u_j'}\right) \tag{11}$$

where $\bar{u}_i$ is the time-averaged velocity, $\bar{p}$ is the time-averaged pressure, μ is the dynamic viscosity of air, and $\rho \overline{u_i' u_j'}$ is the Reynolds stress tensor. The transport equation of the Reynolds stress can be described by,

$$\begin{aligned}
&\frac{\partial}{\partial t}\left(\overline{u_i' u_j'}\right) + \bar{u}_\mathrm{k} \frac{\partial}{\partial x_\mathrm{k}}\left(\overline{u_i' u_j'}\right) \\
&= \underbrace{\frac{\partial}{\partial x_\mathrm{k}}\left[\frac{\nu_\mathrm{t}}{\sigma_\mathrm{k}} \frac{\partial \overline{u_i' u_j'}}{\partial x_\mathrm{k}}\right]}_{D_{\mathrm{T},ij}=\text{Turbulent Diffusion}} \underbrace{-\left[\overline{u_i' u_\mathrm{k}'} \frac{\partial \bar{u}_j}{\partial x_\mathrm{k}} + \overline{u_j' u_\mathrm{k}'} \frac{\partial \bar{u}_i}{\partial x_\mathrm{k}}\right]}_{P_{ij}=\text{Stress Production}} \\
&\underbrace{-C_1 \frac{\varepsilon}{k}\left[\overline{u_i' u_j'} - \frac{2}{3}\delta_{ij} k\right] - C_2\left[P_{ij} - \frac{2}{3}\delta_{ij} P\right]}_{\phi_{ij}=\text{Pressure Strain}} - \underbrace{\frac{2}{3}\delta_{ij}\varepsilon}_{\varepsilon_{ij}=\text{Dissipation}}
\end{aligned} \tag{12}$$

where the production term is given as

$$\begin{aligned}
&P_{ij} = -\left(\overline{u_i' u_\mathrm{k}'} \frac{\partial \bar{u}_j}{\partial x_\mathrm{k}} + \overline{u_j' u_\mathrm{k}'} \frac{\partial \bar{u}_i}{\partial x_\mathrm{k}}\right) \\
&P = \frac{1}{2} P_{ii} \\
&\delta_{ij} = \begin{cases} 1 & (i = j) \\ 0 & (i \neq j) \end{cases}
\end{aligned} \tag{13}$$

In Eq. (12), empirical constants σ_k = 1.0, C_1 = 1.8, and C_2= 0.6. Moreover, the turbulence dissipation rate ε is calculated by the following transport equation,

$$\frac{\partial \varepsilon}{\partial t} + \bar{u}_j \frac{\partial \varepsilon}{\partial x_j} = \frac{\partial}{\partial x_j}\left[\left(\nu + \frac{\nu_\mathrm{t}}{\sigma_\varepsilon}\right)\frac{\partial \varepsilon}{\partial x_j}\right] - C_{\varepsilon 1}\frac{\varepsilon}{k}\overline{u_i' u_j'}\frac{\partial \bar{u}_i}{\partial x_j} - C_{\varepsilon 2}\frac{\varepsilon^2}{k} \tag{14}$$

where empirical constants in Eq. (14) σ_ε = 1.3, $C_{\varepsilon 1}$ = 1.44 and $C_{\varepsilon 2}$ = 1.92.

The discrete particle model (DPM) was used to simulate particle deposition behaviors by tracking each particle trajectory. The particle motion equation can be described by,

$$\begin{aligned}
\frac{\mathrm{d}u_\mathrm{p}}{\mathrm{d}t} &= \frac{1}{\tau}\frac{C_\mathrm{D} Re_\mathrm{p}}{24}(u_\mathrm{g} - u_\mathrm{p}) + \frac{g(\rho_\mathrm{p} - \rho_\mathrm{g})}{\rho_\mathrm{p}} \\
&+ \zeta\sqrt{\frac{\pi S_0}{\Delta t}} + \frac{2\rho K_\mathrm{c} \nu^{0.5}}{\rho_\mathrm{p} d_\mathrm{p}(S_\mathrm{lk} S_\mathrm{kl})} s_{ij}(u - u_\mathrm{p})
\end{aligned} \tag{15}$$

Here, u_g and u_p are the air velocity and particle velocity, respectively. ρ_g and ρ_p are the air density and particle density, respectively. The drag force, the gravity, the buoyancy force, the Brownian force and the Saffman's lift force were considered in the particle motion equation.

The particle relaxation time τ is calculated by,

$$\tau = \frac{S d_\mathrm{p}^2 C_\mathrm{C}}{18\nu} \tag{16}$$

where S is the ratio of particle-to-fluid density. C_C is the Cunningham slip correction factor, which is computed by,

$$C_C = 1 + \frac{2\lambda}{d_p}(1.257 + 0.4e^{-(1.1d_p/2\lambda)}) \tag{17}$$

The drag coefficient C_D is given as,

$$C_D = \frac{24}{Re_p}, \quad \text{for } Re_p < 1 \tag{18}$$

and

$$C_D = \frac{24}{Re_p}(1 + 0.15Re_p^{0.687}), \quad \text{for } 1 < Re_p < 400 \tag{19}$$

When carrying out RANS simulation, it is vital to establish a near-wall model of turbulent duct flow to correctly predict particle deposition (Tian and Ahmadi 2007). A two-layer zonal model with enhanced wall function has usually been adopted to improve the prediction of near-wall turbulence (Tian and Ahmadi 2007). Particle turbulent dispersion induced by turbulent instantaneous fluctuation is also a crucial determinant of particle deposition behaviors. The discrete random walk model (DRW) was recommended by Tian and Ahmadi for the turbulent dispersion of particles (Tian and Ahmadi 2007). The DRW model allows for the successive encounters of particles with turbulent eddies, based on the random velocity fluctuation of fluids with a Gaussian distribution and the time scale of a turbulent eddy (Tian and Ahmadi 2007). The turbulent fluctuating velocity is given as follows:

$$u' = \zeta u'_{\mathrm{rms}},\ v' = \zeta v'_{\mathrm{rms}},\ w' = \zeta w'_{\mathrm{rms}} \tag{20}$$

where ζ is the normal distributed random number with zero mean and unit variance, and u'_{rms}, v'_{rms} and w'_{rms} are the fluctuating velocities obtained using the RSM model. In addition, the wall-normal turbulent fluctuation v'_{rms} in the near-wall region must be corrected for to improve the accuracy of particle turbulent dispersion modeling. To model particle deposition in smooth duct flows, Tian and Ahmadi (2007) recommended correcting for wall-normal fluctuation based on the DNS data obtained by Kim et al. (1987), as follows:

$$\frac{v'_{\mathrm{rms}}}{u^*} = C(y^+)^2 \ \text{ for } \ y^+ < 4 \tag{21}$$

where u^* is frictional velocity and the value of the constant C is suggested to be 0.008. y^+ is the dimensionless distance from the wall, which can be defined as follows:

$$y^+ = \frac{y u^*}{\nu} \tag{22}$$

The summary of numerical models on predicting particle deposition in ventilation duct flow can be seen in the Table 2.

Table 2 Numerical models for particle deposition in ventilation duct flow

Duct airflow	Particle deposition	Advantages	Disadvantages
DNS or LES	DPM	High predicting accuracy	High computational cost
k-ε and k-ω turbulence models	DPM	Low computational cost	Over-prediction of particle deposition velocity
RSM and corrected DRW	DPM	High predicting accuracy, Low computational cost	—

3 Factors influencing particle deposition

In recent years, studies of particle deposition in turbulent duct flows have tended to address more complex duct geometry, such as ribbed duct flows, and more complicated conditions, such as thermal and electric differences. The resulting models of particle deposition are more realistic. This section reviews studies of several important factors influencing particle deposition behaviors, such as duct inclination angle, thermophoresis, electrophoresis and surface ribs. The effects of these factors on particle deposition behaviors and mechanisms, respectively, are presented.

3.1 Effects of inclination angle

Particle deposition commonly occurs in inclined ducts in building ventilation systems and other industrial settings. However, only a few studies have been conducted on this important issue. Recently, You et al. (2012) carefully investigated particle deposition rate in inclined duct airflows through theoretical analysis based on the modified three-layer model, as follows:

$$J = -\left(\varepsilon_p + D\right)\frac{\partial C}{\partial y} - \cos\theta\, v_s C + V_t C \tag{23}$$

where θ is the inclination angle. The influence of inclination angle on particle deposition flux is given as the factor $\cos\theta$. The effects of different surface inclinations and friction velocities on particle deposition rate with different particle sizes were investigated systematically. An empirical equation was proposed based on the researchers' theoretical prediction, and divided into four parts: the fine zone, the coarse zone, the zero zone and the transition zone. Particle deposition characteristics differ between zones. In the fine zone, particle deposition velocity is determined by friction velocity. In the coarse zone, inclination angle is the crucial factor determining particle deposition velocity. In the zero zone, particle deposition velocity is close to zero. The results predicted by the empirical equation were validated using experimental data obtained for a spherical chamber (Cheng 1997).

In addition, Majlesara et al. (2013) investigated particle deposition in an inclined duct using a combination of the V2F turbulent model and the Lagrangian particle trajectory model. The researchers considered Stokes' drag, Saffman's lift force, Brownian force and gravity in their predictions of particle deposition behavior. The effects of different inclination angles on particle deposition rate are displayed in Fig. 3.

Inclination angle was found to have almost no influence on particle deposition velocity for small particles when the particle relaxation time was less than 10^{-3} s, because gravitational settling is not the main mechanism of small particle deposition. However, when the particle relaxation time was longer than 10^{-3} s, particle deposition velocity increased significantly as the duct inclination angle decreased. In this particle size range, gravitational settling played an increasingly important role in particle deposition rate. In the vertical duct case, particle deposition velocity remained almost constant for particle relaxation times longer than 10^{1} s. However, in the inclined and horizontal duct cases, particle deposition velocity continued to increase with particle size. Therefore, the simulation results reported by Majlesara et al. (2013) indicate that inclination angle has a crucial influence on particle deposition for large particles. However, no experimental analysis was conducted to validate the above theoretical analysis and numerical simulation. Future researchers are urged to carry out relevant experimental work on this important issue.

3.2 Effects of thermophoresis

Particles in an air volume with a temperature gradient will experience a force that leads them to migrate in the direction

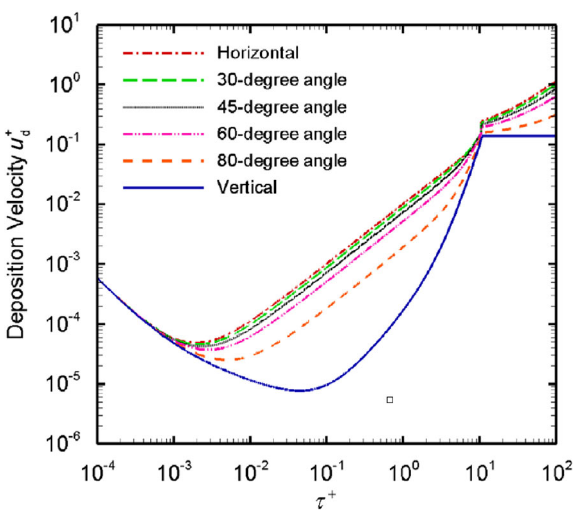

Fig. 3 Particle deposition velocities in duct flow for various inclination angles (Majlesara et al. 2013; reproduced with permission ©Elsevier)

of lower temperature. This motion is known as thermophoresis, and the force exerted on the particles is the thermophoretic force (Zahmatkesh 2008; You and Li 2008; Li and Davis 1995a,b; Montassier et al. 1991; Pratsinis and Kim 1989). The magnitude of the thermophoretic force is determined by the properties of the gas and the particles and the temperature gradient in the air volume (Bakanov 1991). Thermophoresis has wide applications in both natural and industrial processes. It is the result of gas molecules on the warmer side of an air volume striking particles with a greater average momentum than those on the cooler side (Brock 1962). Several studies have been conducted on thermophoresis and the expression of the thermophoretic force. Talbot et al. (1980) recommended calculating the thermophoretic force as follows:

$$F_{\mathrm{th}} = -\frac{3\pi\mu^2 d_{\mathrm{p}} H}{\rho_{\mathrm{a}} T}\frac{\mathrm{d}T}{\mathrm{d}y} \tag{24}$$

where $\mathrm{d}T/\mathrm{d}y$ is the temperature gradient in the air volume and H is the coefficient of the thermophoretic force:

$$H = \left(\frac{2.34}{1+3.42Kn}\right)\left(\frac{k_{\mathrm{a}} / k_{\mathrm{p}} + 2.18Kn}{1+2k_{\mathrm{a}} / k_{\mathrm{p}} + 4.36Kn}\right) \tag{25}$$

Here, k_{a} and k_{p} represent the thermal conductivity of the air and of the particles, respectively. The thermophoretic velocity can thus be obtained as follows:

$$v_{\mathrm{th}} = \frac{-C_{\mathrm{c}} v H}{T}\frac{\mathrm{d}T}{\mathrm{d}y} \tag{26}$$

Thermophoretic velocity can be incorporated into the abovementioned three-layer model to predict particle deposition rate with consideration of the thermophoresis effect. Thermal gradients are common and significant in heating, ventilation and air conditioning (HVAC) ducts, as the air delivered into buildings is usually heated or cooled. He and Ahmadi (1998) numerically investigated the thermophoretic deposition of particles in turbulent duct flows. The results showed that turbulent flow is the dominant mechanism of particle deposition in the bulk flow region, where thermophoresis and the Brownian diffusion of particles can be ignored. However, thermophoresis plays a crucial role in particle deposition behaviors in the viscous sub-layer. In addition, thermophoresis is greatly enhanced by an increase in temperature gradient, in turn affecting particle size range.

Abdolzadeh et al. (2001; 2011a,b,c,d) studied the thermophoretic deposition of particles in turbulent air duct flows using a modified version of the V2F turbulence model. The reported effects of thermophoresis on particle deposition velocity are shown in Fig. 4. As the duct walls were cooled,

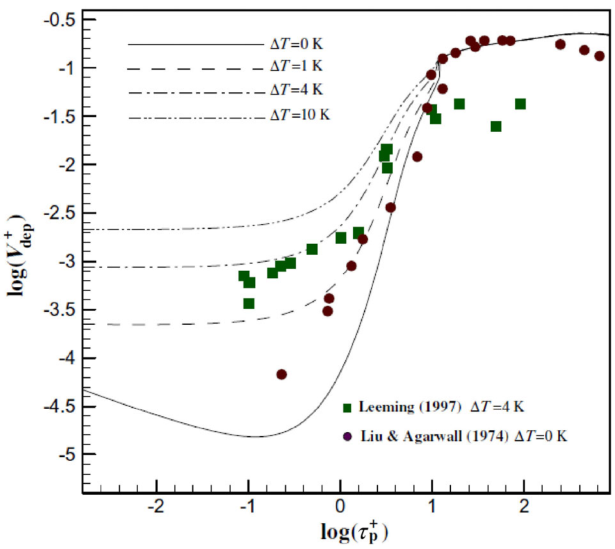

Fig. 4 Effects of thermophoresis on particle deposition velocity in turbulent duct flow (Abdolzadeh et al. 2011e; reproduced with permission ©Elsevier)

the thermophoretic force was directed toward the walls. Particle deposition velocity increased greatly, by about two orders of magnitude, for small particles ($\tau_p^+<1$). However, thermophoresis had almost no effect on particle deposition velocity for the large particles ($\tau_p^+>1$). The numerical results reported by Abdolzadeh et al. (2011a,b,c,d,e) agree well with the experimental data obtained by Leeming (1997). This indicates that numerical simulation can accurately predict the thermophoresis effect on particle deposition in turbulent duct flows. However, most studies of thermophoresis to date have been based on theoretical analysis and/or numerical simulation. Experimental studies of the effects of thermophoresis on particle deposition are still limited.

3.3 Effects of electrophoresis

Charged particles in gas subject to electric fields experience an electrostatic force. The migration of particles caused by this force is known as electrophoresis. The electrostatic force exerted on a charged particle near a conducting surface can be calculated as follows (Cooper et al. 1989; Fan and Ahmadi 1994; Hartmann et al. 1976; Hidv 1984; Soltani and Ahmadi 1999):

$$F_e = qE - \frac{q^2}{16\pi\varepsilon_o y^2} + \frac{qEd_p^3}{16y^3} - \frac{3\pi\varepsilon_o d_p^6 E}{128y^4} \tag{27}$$

where $\varepsilon_o = 8.86\times10^{-12}\ C^2{\cdot}N^{-1}{\cdot}m^{-2}$ is the permittivity of air. The terms on the right-hand side of Eq. (27) represent the Coulomb force, the image force, the dielectric force and the dipole-dipole force, respectively. These forces are induced by the electric field, an image charge of $-q$ at position $-y$ from the surface, the gradient of the field from the image charge and the interaction between the induced dipole and its image, respectively. The dielectric force and the dipole-dipole force are likely to be negligible compared with the Coulomb force, according to He and Ahmadi (1999). Electrophoresis plays a crucial role in particle removal and air cleaning by devices such as air electrostatic precipitators (ESPs) (Vincent and MacLennan 1980; Suh and Kim 1996). In renewable energy applications such as solar PV panels, the electrophoresis of dust particles in the air is induced by electric fields generated by solar PV systems (Jiang et al. 2016). In HVAC ducts, no significant electric fields can appear due to the use of electrically conducting materials. Therefore, the electrophoresis of particles in HVAC ducts is not obvious (Sippola and Nazaroff 2004).

The electrophoretic deposition of particles in turbulent air duct flows was investigated by Abdolzadeh et al. (2011a,b,c,d,e) using a modified version of the V2F turbulence model. The observed effects of electrophoresis on particle deposition velocity are shown in Fig. 5.

Figure 5 shows that particle deposition velocity was significantly increased by electrophoresis. However, the influence of electrophoresis on aerosol particles differed with particle size. For small particles ($\tau_p^+<1$), deposition velocity was significantly enhanced by electrophoresis. However, the deposition velocities of large particles ($\tau_p^+>1$) were almost unaffected by electrophoresis. Therefore, similar to thermophoresis, electrophoresis has a more intense influence on deposition behaviors for small particles. Future researchers are encouraged to conduct accurate experimental studies of electrophoresis.

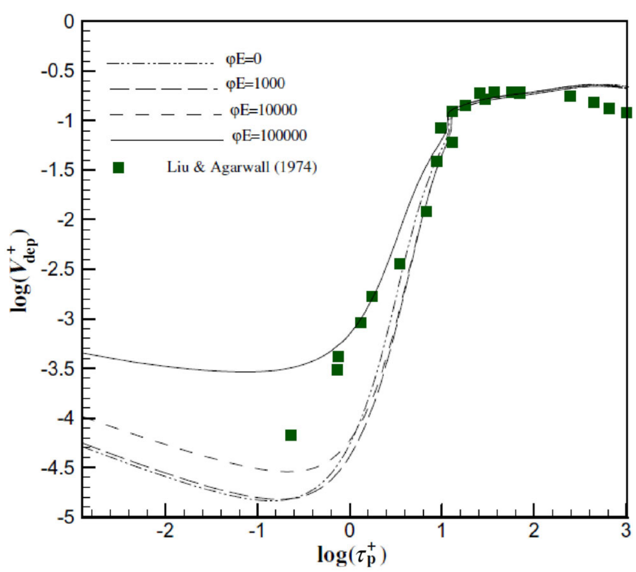

Fig. 5 Effect of electrophoresis on particle deposition velocity in turbulent duct flows (Abdolzadeh et al. 2011e; reproduced with permission ©Elsevier)

3.4 Effects of surface ribs

In a large number of air-cleaning devices, particle deposition enhancement is necessary and significant to improve aerosol removal efficiency and performance. Surface ribs have been found to be an effective and efficient means of enhancing particle deposition (Lo Iacono et al. 2005; Barth et al. 2013). For example, surface ribs can be used in ESPs to increase particle collection efficiency (Lecrivain et al. 2014; Liou et al. 1993; Okamoto et al. 1993). However, the optimization of surface rib size and arrangement needs to be investigated carefully. Lu et al. (Lu and Lu 2015b,c, 2016; Lu et al. 2016, 2017) investigated the effects of rib spacing, height, shape and arrangement on particle deposition enhancement in turbulent duct flows. They also discussed and analyzed the detailed mechanisms of particle deposition enhancement by surface ribs. Figure 6 shows the effects of different surface rib spacings and heights on particle deposition velocities in turbulent duct flows. Particle deposition velocity was found to be greatly enhanced—by several orders of magnitude—by surface ribs. However, the degree of enhancement of deposition velocity differed significantly between particles with different relaxation times. When the particles were small ($\tau_p^+<1$), particle deposition velocity was enhanced by about four orders of magnitude by the surface ribs. However, deposition velocity was enhanced by only about two orders of magnitude for large particles ($\tau_p^+>1$).

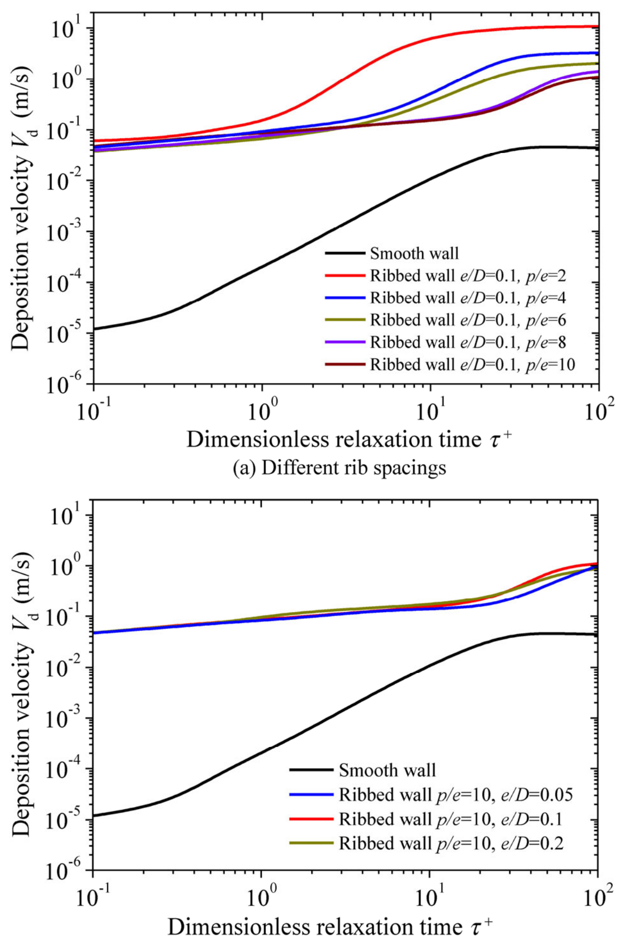

Fig. 6 Particle deposition velocity in ribbed duct flow with different rib spacings and heights (Lu and Lu 2015b; reproduced with permission ©Elsevier)

The mechanisms of particle deposition enhancement by surface ribs were also discussed and analyzed by Lu et al. (Lu and Lu 2015b,c, 2016; Lu et al. 2016, 2017). In addition to interception by windward rib surfaces and increased deposition area, the entrainment of turbulent eddies induced by the surface ribs was found to be the main mechanism of small particle deposition. The turbulent structures in ribbed ducts are quite different from those in smooth ducts. In the latter case, the flow is along the streamwise direction and the value of turbulence kinetic energy (TKE) near the wall is very small. In ribbed ducts, small particles are easily captured by the vortices in the rib cavity and then entrained for deposition on the rib surface or walls. Higher values of TKE near the surface ribs are observed in ribbed than in smooth duct flows. Therefore, the arrangement of surface ribs is an efficient and effective way of enhancing particle deposition, especially for small particles.

5 Conclusions

The characteristics of particle deposition in turbulent duct flows were reviewed in this paper. The main mechanisms of particle deposition in smooth duct flows are turbophoresis, Brownian diffusion, turbulent diffusion and gravitational settling. Numerical simulation was shown to have become the most powerful method. However, experimental measurement is essential to validate numerical results. Developing a theoretical model to accurately predict particle deposition in complex turbulent duct flows is challenging. The influencing factors, such as duct inclination angle, thermophoretic deposition, electrophoretic deposition and surface ribs, have a more significant influence on small particle deposition. However, their influence on large particle deposition behaviors was much more limited due to large particle inertia.

Particle deposition in complicated three-dimensional duct flows offers a promising direction for future research. Moreover, researchers are urged to conduct experimental measurements of particle deposition velocity and characteristics to validate their numerical results.

Acknowledgements

The authors appreciate the financial supports provided by “Xinghua Scholar Talents Plan”of South China University of Technology (K5183300), The Hong Kong Polytechnic University Postdoctoral Fellowships Scheme (G-YW0K) and Shenzhen Peacock Plan (KQTD2015071616442225).

References

Abdolzadeh M, Mehrabian MA, Zahedi G, Soltani Goharrizi A (2011a). Numerical study to predict the particle deposition under the influence of operating forces on a tilted surface in the turbulent flow. *Advanced Powder Technology*, 22: 405–415.

Abdolzadeh M, Mehrabian MA (2011b). Combined effect of thermophoretic force and other influencing parameters on the particle deposition rate on a tilted rough surface. *International Journal of Thermal Sciences*, 50: 954–964.

Abdolzadeh M, Mehrabian MA, Soltani Goharrizi A (2011c). Predicting the particle deposition characteristics using a modified Eulerian method on a tilted surface in the turbulent flow. *Particulate Science and Technology*, 29: 503–525.

Abdolzadeh M, Mehrabian MA, Akbarinia A (2011d). Application of a modified Eulerian model to study the particle deposition on a vertical surface in turbulent flow. *Powder Technology*, 214: 83–88.

Abdolzadeh M, Mehrabian MA, Soltani Goharrizi A (2011e). Effect of thermophoresis and other parameters on the particle deposition on a tilted surface. *International Journal of Heat and Fluid Flow*, 32: 670–679.

Bakanov SP (1991). Thermophoresis in gases at small knudsen numbers. *Aerosol Science and Technology*, 15: 77–92.

Barth T, Reiche M, Banowski M, Oppermann M, Hampel U (2013). Experimental investigation of multilayer particle deposition and resuspension between periodic steps in turbulent flows. *Journal of Aerosol Science*, 64: 111–124.

Blocken B (2018). LES over RANS in building simulation for outdoor and indoor applications: A foregone conclusion? *Building Simulation*, 11: 821–870.

Brock JR (1962). On the theory of thermal forces acting on aerosol particles. *Journal of Colloid Science*, 17: 768–780.

Caporaloni M, Tampieri F, Trombetti F, Vittori O (1975). Transfer of particles in nonisotropic air turbulence. *Journal of the Atmospheric Sciences*, 32: 565–568.

Chen Q, Zhang Z (2005). Prediction of particle transport in enclosed environment. *China Particuology*, 3: 364–372.

Chen Q (2009). Ventilation performance prediction for buildings: A method overview and recent applications. *Building and Environment*, 44: 848–858.

Cheng YS (1997). Wall deposition of radon progeny and particles in a spherical chamber. *Aerosol Science and Technology*, 27: 131–146.

Cooper DW, Peters MH, Miller RJ (1989). Predicted deposition of submicronmeter particles due to diffusion and electrostatics in viscous axisymmetric stagnation-point flow. *Aerosol Science and Technology*, 11: 133–143.

El-Shobokshy MS (1983). Experimental measurements of aerosol deposition to smooth and rough surfaces. *Atmospheric Environment*, 17: 639–644.

Fan FG, Ahmadi G (1994). On the sublayer model for turbulent deposition of aerosol particles in the presence of gravity and electric fields. *Aerosol Science and Technology*, 21: 49–71.

Friedlander SK, Johnstone HF (1957). Deposition of suspended particles from turbulent gas streams. *Industrial and Engineering Chemistry*, 49: 1151–1156.

Gao NP, Niu JL (2007). Modeling particle dispersion and deposition in indoor environments. *Atmospheric Environment*, 41: 3862–3876.

Gao N, Niu J, He Q, Zhu T, Wu J (2012). Using RANS turbulence models and Lagrangian approach to predict particle deposition in turbulent channel flows. *Building and Environment*, 48: 206–214.

Gao J, Zeng L, Cao C, Ye W, Zhang X (2018). Multi-objective optimization for sensor placement against suddenly released contaminant in air duct system. *Building Simulation*, 11: 139–153.

Guha A (2008). Transport and deposition of particles in turbulent and laminar flow. *Annual Review of Fluid Mechanics*, 40: 311–341.

Hahn LA, Stukel JJ, Leong KH, Hopke PK (1985). Turbulent deposition of submicron particles on rough walls. *Journal of Aerosol Science*, 16: 81–86.

Hartmann GC, Marks LM, Yang CC (1976). Physical models for photoactive pigment electrophotography. *Journal of Applied Physics*, 47: 5409–5420.

He C, Ahmadi G (1998). Particle deposition with thermophoresis in laminar and turbulent duct flows. *Aerosol Science and Technology*, 29: 525–546.

He C, Ahmadi G (1999). Particle deposition in a nearly developed turbulent duct flow with electrophoresis. *Journal of Aerosol Science*, 30: 739–758.

Hidy GM (1984). Aerosols: An Industrial and Environmental Science. New York: Academic Press.

Jiang H, Lu L, Sun K (2010). Simulation of particle deposition in ventilation duct with a particle-wall impact model. *Building and Environment*, 45: 1184–1191.

Jiang H, Lu L, Sun K (2011). Experimental study and numerical investigation of particle penetration and deposition in 90° bent ventilation ducts. *Building and Environment*, 46: 2195–2202.

Jiang H, Lu L, Sun K (2012). Computational fluid dynamics (CFD) modelling of particle deposition in a two-dimensional turbulent channel air flow: Study of influence factors. *Indoor and Built Environment*, 21: 264–272.

Jiang Y, Lu L, Lu H (2016). A novel model to estimate the cleaning frequency for dirty solar photovoltaic (PV) modules in desert environment. *Solar Energy*, 140: 236–240.

Kallio GA, Reeks MW (1989). A numerical simulation of particle deposition in turbulent boundary layers. *International Journal of Multiphase Flow*, 15: 433–446.

Kato S, Yang JH (2008). Study on inhaled air quality in a personal air-conditioning environment using new scales of ventilation efficiency. *Building and Environment*, 43: 494–507.

Kim J, Moin P, Moser R (1987). Turbulence statistics in fully developed channel flow at low Reynolds number. *Journal of Fluid Mechanics*, 177: 133–166.

Lai ACK, Byrne MA, Goddard AJH (1999). Measured deposition of aerosol particles on a two-dimensional ribbed surface in a turbulent duct flow. *Journal of Aerosol Science*, 30: 1201–1214.

Lai ACK, Nazaroff WW (2000). Modeling indoor particle deposition from turbulent flow onto smooth surfaces. *Journal of Aerosol Science*, 31: 463–476.

Lai ACK, Byrne MA, Goddard AJH (2000). Enhanced particle loss in ventilation duct with ribbed surface. *Building and Environment*, 35: 425–432.

Lai ACK, Byrne MA, Goddard AJH (2001). Aerosol deposition in turbulent channel flow on a regular array of three-dimensional roughness elements. *Journal of Aerosol Science*, 32: 121–137.

Lai ACK (2002). Particle deposition indoors: A review. *Indoor Air*, 12: 211–214.

Lai ACK, Byrne MA, Goddard AJH (2002). Particle deposition in ventilation duct onto three-dimensional roughness elements. *Building and Environment*, 37: 939–945.

Lai ACK (2005). Modeling indoor coarse particle deposition onto smooth and rough vertical surfaces. *Atmospheric Environment*, 39: 3823–3830.

Lai ACK, Nazaroff WW (2005). Supermicron particle deposition from turbulent chamber flow onto smooth and rough vertical surfaces. *Atmospheric Environment*, 39: 4893–4900.

Lai ACK, Chen FZ (2006). Modeling particle deposition and distribution in a chamber with a two-equation Reynolds-averaged Navier-Stokes model. *Journal of Aerosol Science*, 37: 1770–1780.

Lecrivain G Sevan D-M, Thomas B, Hampel U (2014). Numerical simulation of multilayer deposition in an obstructed channel flow. *Advanced Powder Technology*, 25: 310–320.

Leeming AD (1997). Particle deposition from turbulent flows. PhD Thesis, Cambridge University, UK.

Lee KW, Gieseke JA (1994). Deposition of particles in turbulent pipe flows. *Journal of Aerosol Science*, 25: 699–709.

Li A, Ahmadi G (1992). Dispersion and deposition of spherical particles from point sources in a turbulent channel flow. *Aerosol Science and Technology*, 16: 209–226.

Li A, Ahmadi G (1993). Deposition of aerosols on surfaces in a turbulent channel flow. *International Journal of Engineering Science*, 31: 435–451.

Li A, Ahmadi G (1995). Computer simulation of particle deposition in the upper tracheobronchial tree. *Aerosol Science and Technology*, 23: 201–223.

Li W, Davis EJ (1995a). Measurement of the thermophoretic force by electrodynamic levitation: Microspheres in air. *Journal of Aerosol Science*, 26: 1063–1083.

Li W, Davis EJ (1995b). The effects of gas and particle properties on thermophoresis. *Journal of Aerosol Science*, 26: 1085–1099.

Liou TM, Hwang JJ, Chen SH (1993). Simulation and measurement of enhanced turbulent heat transfer in a channel with periodic ribs on one principal wall. *International Journal of Heat and Mass Transfer*, 36: 507–517.

Liu BYH, Agarwal JK (1974). Experimental observation of aerosol deposition in turbulent flow. *Journal of Aerosol Science*, 5: 145–155.

Lo Iacono G, Tucker PG, Reynolds AM (2005). Predictions for particle deposition from LES of ribbed channel flow. *International Journal of Heat and Fluid Flow*, 26: 558–568.

Lu H, Lu L (2015a). Numerical investigation on particle deposition enhancement in duct air flow by ribbed wall. *Building and Environment*, 85: 61–72.

Lu H, Lu L (2015b). Effects of rib spacing and height on particle deposition in ribbed duct air flows. *Building and Environment*, 92: 317–327.

Lu H, Lu L (2015c). A numerical study of particle deposition in ribbed duct flow with different rib shapes. *Building and Environment*, 94: 43–53.

Lu H, Lu L (2016). CFD investigation on particle deposition in aligned and staggered ribbed duct air flows. *Applied Thermal Engineering*, 93: 697–706.

Lu H, Lu L, Jiang Y (2016). Numerical simulation of particle deposition in duct air flows with uniform, expanding or contracting cross-section. *Energy and Buildings*, 128: 867–875.

Lu H, Lu L, Jiang Y (2017). Numerical study of monodispersed particle deposition rates in variable-section ducts with different expanding or contracting ratios. *Applied Thermal Engineering*, 110: 150–161.

Majlesara M, Salmanzadeh M, Ahmadi G (2013). A model for particles deposition in turbulent inclined channels. *Journal of Aerosol Science*, 64: 37–47.

Montassier N, Boulaud D, Renoux A (1991). Experimental study of thermophoretic particle deposition in laminar tube flow. *Journal of Aerosol Science*, 22: 677–687.

Nazaroff WW (2004). Indoor particle dynamics. *Indoor Air*, 14: 175–183.

Nazaroff WW (2008). Inhalation intake fraction of pollutants from episodic indoor emissions. *Building and Environment*, 43: 269–277.

Okamoto S, Seo S, Nakaso K, Kawai I (1993). Turbulent shear flow and heat transfer over the repeated two-dimensional square ribs on ground plane. *Journal of Fluids Engineering*, 115: 631–637.

Ounis H, Ahmadi G, McLaughlin JB (1993). Brownian particle deposition in a directly simulated turbulent channel flow. *Physics of Fluids A: Fluid Dynamics*, 5: 1427–1432.

Piskunov VN (2009). Parameterization of aerosol dry deposition velocities onto smooth and rough surfaces. *Journal of Aerosol Science*, 40: 664–679.

Postma AK, Schwendiman LC (1960). Studies in micrometrics: I. Particle deposition in conduits as a source of error in aerosol sampling. Report HW-65308, Richland, Washington: Hanford Laboratory.

Pratsinis SE, Kim KS (1989). Particle coagulation, diffusion and thermophoresis in laminar tube flows. *Journal of Aerosol Science*, 20: 101–111.

Roff MW (1994). A novel lighting system for the measurement of dermal exposure using a fluorescent dye and an image processor. *Annals of Occupational Hygiene*, 38: 903–919.

Sehmel GA (1970). Particle deposition from turbulent air flow. *Journal of Geophysical Research*, 75: 1766–1781.

Shimada M, Okuyama K, Asai M (1993). Depostition of submicron aerosol particles in turbulent and transitional flow. *AIChE Journal*, 39: 17–26.

Sippola MR, Nazaroff WW (2004). Experiments measuring particle deposition from fully developed turbulent flow in ventilation ducts. *Aerosol Science and Technology*, 38: 914–925.

Soltani M Mehdi S, Ahmadi G (1999). Charged particle trajectory statistics and deposition in a turbulent channel flow. *Aerosol Science and Technology*, 31: 170–186.

Suh YJ, Kim SS (1996). Effect of obstructions on the particle collection efficiency in a two-stage electrostatic precipitator. *Journal of Aerosol Science*, 27: 61–74.

Sun W, Ji J, Li Y, Xie X (2007). Dispersion and settling characteristics of evaporating droplets in ventilated room. *Building and Environment*, 42: 1011–1017.

Sun K, Lu L, Jiang H (2011a). Modelling of particle deposition and rebound behaviour on ventilation ducting wall using an improved wall model. *Indoor and Built Environment*, 20: 300–312.

Sun K, Lu L, Jiang H (2011b). A computational investigation of particle distribution and deposition in a 90° bend incorporating a particle-wall model. *Building and Environment*, 46: 1251–1262.

Sun K, Lu L, Jiang H (2012). A numerical study of bend-induced particle deposition in and behind duct bends. *Building and Environment*, 52: 77–87.

Sun K, Lu L, Jiang H, Jin HH (2013). Experimental study of solid particle deposition in 90 ventilated bends of rectangular cross section with turbulent flow. *Aerosol Science and Technology*, 47: 115–124.

Sun K, Lu L (2013). Particle flow behavior of distribution and deposition throughout 90° bends: Analysis of influencing factors. *Journal of Aerosol Science*, 65: 26–41.

Tian L, Ahmadi G (2007). Particle deposition in turbulent duct flows—Comparisons of different model predictions. *Journal of Aerosol Science*, 38: 377–397.

Talbot L, Cheng RK, Schefer RW, Willis DR (1980). Thermophoresis of particles in a heated boundary layer. *Journal of Fluid Mechanics*, 101: 737–758.

Tian ZF, Tu JY, Yeoh GH, Yuen RKK (2007). Numerical studies of indoor airflow and particle dispersion by large eddy simulation. *Building and Environment*, 42: 3483–3492.

Vincent JH, MacLennan ASM (1980). Aerodynamic considerations in electrostatic precipitaton. *Journal of Electrostatics*, 8: 325–342.

Wang L, Chen Q (2007). Theoretical and numerical studies of coupling multizone and CFD models for building air distribution simulations. *Indoor Air*, 17: 348–361.

Wells AC, Chamberlain AC (1967). Transport of small particles to vertical surfaces. *British Journal of Applied Physics*, 18: 1793–1799.

Wood NB (1981). A simple method for the calculation of turbulent deposition to smooth and rough surfaces. *Journal of Aerosol Science*, 12: 275–290.

Wu Y, Niu J, Liu X (2018). Air infiltration induced inter-unit dispersion and infectious risk assessment in a high-rise residential building. *Building Simulation*, 11: 193–202.

You C, Li G (2008). Direct numerical simulation of microparticle motion in channel flow with thermophoresis. *Journal of Environmental Engineering*, 134: 138–144.

You R, Zhao B, Chen C (2012). Developing an empirical equation for modeling particle deposition velocity onto inclined surfaces in indoor environments. *Aerosol Science and Technology*, 46: 1090–1099.

Zahmatkesh I (2008). On the importance of thermophoresis and Brownian diffusion for the deposition of micro- and nanoparticles. *International Communications in Heat and Mass Transfer*, 35: 369–375.

Zhai Z, Jin Q (2018). Identifying decaying contaminant source location in building HVAC system using the adjoint probability method. *Building Simulation*, 11: 1029–1038.

Zhang HF, Ahmadi G (2000). Aerosol particle transport and deposition in vertical and horizontal turbulent duct flows. *Journal of Fluid Mechanics*, 406: 55–80.

Zhang Z, Chen Q (2007). Comparison of the Eulerian and Lagrangian methods for predicting particle transport in enclosed spaces. *Atmospheric Environment*, 41: 5236–5248.

Zhao B, Zhang Z, Li X (2005). Numerical study of the transport of droplets or particles generated by respiratory system indoors. *Building and Environment*, 40: 1032–1039.

Zhao B, Wu J (2006a). Modeling particle deposition from fully developed turbulent flow in ventilation duct. *Atmospheric Environment*, 40: 457–466.

Zhao B, Wu J (2006b). Modeling particle deposition onto rough walls in ventilation duct. *Atmospheric Environment*, 40: 6918–6927.

Zhao B, Yang C, Yang X, Liu S (2008). Particle dispersion and deposition in ventilated rooms: Testing and evaluation of different Eulerian and Lagrangian models. *Building and Environment*, 43: 388–397.

Zhao Y, Zhao B (2018). Emissions of air pollutants from Chinese cooking: A literature review. *Building Simulation*, 11: 977–995.